HHS Public Access

Author manuscript

Mol Cancer Ther. Author manuscript; available in PMC 2024 August 01.

Published in final edited form as:

Mol Cancer Ther. 2024 February 01; 23(2): 223–234. doi:10.1158/1535-7163.MCT-23-0173.

SKP2 knockout in Rb1/p53 deficient mouse models of osteosarcoma induces immune infiltration and drives a transcriptional program with a favorable prognosis

Alexander Ferrena[*,1,2], **Jichuan Wang**[*,3], **Ranxin Zhang**[*,3], **Burcu Karadal-Ferrena**[4], **Waleed Al-Hardan**[3], **Swapnil Singh**[3], **Hasibagan Borjihan**[3], **Edward L. Schwartz**[5,6,7], **Hongling Zhao**[8], **Maja H. Oktay**[4,9,10,11], **Rui Yang**[3], **David S Geller**[3], **Bang H Hoang**[†,3], **Deyou Zheng**[†,2,12,13]

[1]Institute for Clinical and Translational Research, Albert Einstein College of Medicine, Bronx, NY, USA

[2]Department of Genetics, Albert Einstein College of Medicine, Bronx, NY, USA

[3]Department of Orthopedic Surgery, Montefiore Medical Center, Albert Einstein College of Medicine, Bronx, NY, USA

[4]Department of Pathology, Albert Einstein College of Medicine, Bronx, NY, USA

[5]Department of Oncology, Albert Einstein College of Medicine, Bronx, NY, USA

[6]Department of Medicine, Albert Einstein College of Medicine, Bronx, NY, USA

[7]Department of Molecular Pharmacology, Albert Einstein College of Medicine, Bronx, NY, USA

[8]Department of Developmental & Molecular Biology, Albert Einstein College of Medicine, Bronx, NY, USA

[9]Department of Surgery, Montefiore Medical Center, Albert Einstein College of Medicine, Bronx, NY, USA.

[10]Gruss-Lipper Biophotonics Center, Montefiore Medical Center, Albert Einstein College of Medicine, Bronx, NY, USA

[11]Integrated Imaging Program, Montefiore Medical Center, Albert Einstein College of Medicine, Bronx, NY, USA

[12]Department of Neurology, Albert Einstein College of Medicine, Bronx, NY, USA

[13]Department of Neuroscience, Albert Einstein College of Medicine, Bronx, NY, USA

[†]Corresponding authors: Deyou Zheng, Ph.D., Albert Einstein College of Medicine, 1301 Morris Park Ave, Bronx, NY 10461, deyou.zheng@einsteinmed.edu, Bang H. Hoang, M.D., Department of Orthopedic Surgery, Montefiore Medical Center, Albert Einstein College of Medicine, Bronx, NY 10461, bahoang@montefiore.org.

[*]These authors contributed equally to this work.

Author Contributions

A.F. performed bioinformatic and clinical data analysis. J.W. performed tumor isolation and RNA-seq analysis. R.Z. performed RT-PCR and IHC assays. B.K.F. and M.H.O. assisted with IHC quantification and analysis. W.A.H, S.S., and H.B. assisted with mouse model preparation and tumor isolation. E.S. and H.Z. assisted with data interpretation. R.Y. and D.G. assisted with clinical data analysis and data interpretation. B.H. and D.Z. conceived the study, supervised all work, and acquired funding. D.Z. supervised all data analysis. A.F., B.H. and D.Z. wrote the manuscript with inputs from all authors.

Conflict of Interest: The authors declare no potential conflicts of interest.

Abstract

Osteosarcoma (OS) is an aggressive bone malignancy with a poor prognosis. One putative proto-oncogene in OS is *SKP2*, encoding a substrate recognition factor of the SCF E3 ubiquitin ligase. We previously demonstrated that *SKP2* knockout in murine OS improved survival and delayed tumorigenesis. Here we performed RNA-sequencing (RNA-seq) on tumors from a transgenic OS mouse model with conditional *Trp53* and *Rb1* knockouts in the osteoblast lineage ("DKO": Osx1-Cre;$Rb1^{lox/lox}$;$p53^{lox/lox}$) and a triple-knockout model with additional *Skp2* germline knockout ("TKO": Osx1-Cre;$Rb1^{lox/lox}$;$p53^{lox/lox}$;$SKP2^{-/-}$), followed by qPCR and immunohistochemistry validation. To investigate the clinical implications of our results, we analyzed a human OS patient cohort ("NCI-TARGET OS") with RNA-seq and clinical data. We found large differences in gene expression after SKP2 knockout. Surprisingly, we observed increased expression of genes related to immune microenvironment infiltration in TKO tumors, especially the signature genes for macrophages and to a lesser extent, T cells, B cells and vascular cells. We also uncovered a set of relevant transcription factors that may mediate these changes. In OS patient cohorts, high expression of genes upregulated in TKO was correlated with favorable overall survival, which was largely explained by the macrophage gene signatures. This relationship was further supported by our finding that SKP2 expression was negatively correlated with macrophage infiltration in the NCI-TARGET OS and the TCGA Sarcoma cohorts. Overall, our findings indicate that SKP2 may mediate immune exclusion from the OS tumor microenvironment, suggesting that SKP2 modulation in OS may induce anti-tumor immune activation.

Keywords

Osteosarcoma; SKP2; RNA-seq; TME; Immune infiltration

Introduction

Osteosarcoma (OS) is a cancer of bone tissue defined by mesenchymal cell histology and deposition of bone matrix[1,2]. OS is the most common pediatric bone malignancy with annual US incidence of 3.1 cases per million[3]. Disease progression commonly involves metastasis to lungs[4]. For non-metastatic cases at diagnosis, 5-year survival is 70% while for metastatic cases, comprising 15 to 25% of incidents, the rate is 30% [4,5]. Genetically, OS is complex and involves many DNA copy number alterations, but the two most frequent mutations are loss of the tumor suppressors *TP53* and *RB1* [6–10]. *In vivo* investigation in preclinical murine models revealed that ablation of *Trp53* and *Rb1* by *Osterix (Osx)*-driven Cre-Lox genetic recombination generates bone tumors that strongly resemble human OS in histology, cytogenetics, and metastatic progression[11]. Our recent analysis of clinical genomic datasets revealed that *TP53* and *RB1* were respectively the first and second most frequently mutated genes in OS and furthermore were often co-mutated[12].

S-phase Kinase Associated Protein 2 (*SKP2*) codes for an F-box substrate recognition factor of the Skp1-Cullin1-F-box (SCF) E3 ubiquitin ligase complex. Its known functions include activation of cell cycle, cell growth, and migration, along with repression of apoptosis[13]. Two key targets for proteolytic ubiquitination by SCF^{SKP2} are the cyclin-dependent kinase inhibitors p21 and p27, allowing cell cycle progression[14,15]. In mouse models of pituitary

and prostate cancers with *Rb1* and *Trp53* loss, *Skp2* knockout was shown to be synthetic-lethal, permanently blocking tumorigenesis in a p27-mediated manner[16]. Mechanistically, *SKP2* inactivation in the context of *Rb1* deficiency did not block proliferation, but instead resulted in p27-mediated apoptosis[17]. Specifically, *Rb1* deletion induced activation of the transcription factor *E2f1* resulting in proliferative gene expression, but co-deletion of *Rb1* and *Skp2* allowed accumulated p27 to form more Cyclin A-p27 complex, which releases the restraining effects of Cyclin A on *E2f1*, causing *E2f1* "superactivation" and resulting in p53-independent apoptosis and blockage of tumorigenesis[18]. SKP2 thus represents an attractive and targetable oncogene in OS and other cancers driven by *RB1* and *P53* mutations. However, in other contexts such as *Myc*-driven lymphomagenesis, SKP2 inhibition showed little effect[19].

Pharmacologic inhibitors of SKP2 include Pevonedistat, an inhibitor of neddylation, a key upstream post-translation modification required for SCF^{SKP2} and other cullin-RING E3 ligases[20]. Other, more specific inhibitors include "C1", which blocks the SKP2-p27 interaction, and "C25", which blocks SKP2's interaction with SKP1 that is required for SCF's E3 ubiquitylation activity[21,22]. Our previous work has demonstrated that pharmacologic inhibition of SKP2 reduced invasion and lung metastasis in patient-derived xenograft OS models [23]. Additionally, blocking the proteolytic ubiquitination of p27 by SKP2 in a mouse model of OS with either genetic or pharmacologic methods promoted survival and induced apoptosis and cell cycle arrest[12]. Most recently, we have shown that genetic knockout and pharmacologic inhibition of SKP2 further improved survival and promoted tumor apoptosis in the mouse DKO OS model[24]. However, unlike in models of pituitary and prostate cancers, OS tumors with SKP2 knockout continue to develop and progress, suggesting undescribed context-specific resistance mechanisms. Additionally, despite the importance of SKP2 to cell proliferation and cancers, to our knowledge no data on the impact of SKP2 knockout on the transcriptome has been reported.

Immune and stromal infiltration into the tumor microenvironment (TME) is widely recognized as a key characteristic of solid tumor malignancies. Single-cell RNA-seq (scRNA-seq) studies have reported a diverse ecosystem of infiltrating non-malignant cell populations within OS tumors[25,26]. While OS frequently presents with genomic instability resulting in neoantigens, OS tumors were found to employ mechanisms of lymphocyte exclusion, and checkpoint inhibitors failed to show clinical benefits[27–29]. Macrophages are consistently observed in the TME of many solid malignancies including OS[25,26]. In OS, macrophage infiltration has been shown to be correlated with improved metastasis-free survival[30]. Several recent pre-clinical studies have reported success with macrophage-based immunotherapy for OS[31,32]. However, not all prior reports consistently show macrophages portend a positive prognosis in OS[33]. Taken together, the literature indicates that macrophages are a complex, context-dependent component of the TME that may be activated for anti-tumor activity in OS and other malignancies.

Here, we set out to study the transcriptional regulatory roles of SKP2 in OS using murine models. As transgenic mouse models are immunologically intact and give rise to autochthonous tumors, they more closely resemble clinical presentation of OS than cell culture or transplanted tumor models. We compared OS models with germline SKP2

knockout and control using RNA-seq and bioinformatics analysis. Surprisingly, we found that SKP2 knockout drove immune cell (T cell and macrophage) recruitment to the OS TME. Additionally, genes with increased expression upon SKP2 knockout correlated with a significant survival benefit in OS patients in a manner likely driven by macrophage infiltration. Moreover, SKP2 was negatively correlated with macrophage infiltration in OS and soft tissue sarcoma patients. Thus, for the first time, we have uncovered evidence that SKP2 may act as a mediator of immune exclusion from the OS tumor microenvironment.

Materials and Methods

Establishment of animal models

Osx1-Cre mice, $Rb1^{lox/lox}$ mice, $Trp53^{lox/lox}$ mice, and $Skp2^{-/-}$ mice were described previously[11,12,34]. All mice used for experiments are on FVB, C57BL6J, and 129Sv hybrid backgrounds. First, $Rb1^{lox/lox}$ mice were crossed with $Trp53^{lox/lox}$ mice to generate $Trp53^{lox/lox}$, $Rb1^{lox/lox}$, mice, and were further crossed with Osx1-Cre mice to generate Osx1-Cre; $Trp53^{lox/lox}$, $Rb1^{lox/lox}$ mice. The $Skp2^{-/-}$ mice were crossed with Osx1-Cre;$Trp53^{lox/lox}$,$Rb1^{lox/lox}$ mice to generate Osx1-Cre;$Rb1^{lox/lox}$;$Trp53^{lox/lox}$; $Skp2^{-/-}$ mice. Animals were maintained under a pathogen-free condition in the Albert Einstein College of Medicine animal facility. Animal experimental protocols were reviewed and approved by Einstein Animal Care and Use Committee (#20180401), conforming to accepted standards of humane animal care. The tumor diameter was measured using a caliper every three days, and the relative tumor volume was calculated by the following formula: (length x $width^2$) x 0.526. Tumors were resected when the volumes reached approximately 500 mm^3.

RNA-sequencing

Mouse tumor tissues from DKO or TKO animals were harvested and processed for RNA-seq (Supplementary Table 1). Approximately 100 mg of fresh tumor tissue was collected and processed using the RNeasy Mini Kit (#74104 Qiagen) for RNA extraction following the manufacturer's protocol. Samples were first quantified and then evaluated for RNA integrity, degradation, and contamination. Next, the rRNA-depleted RNA sample was enriched using oligo(dT) beads and randomly fragmented, followed by standard library preparation for sequencing using the Illumina HiSeq platform. Paired-end sequencing (150-bp) data were processed by the Illumina pipeline, and the resulting RNA-seq reads were mapped to the mouse reference genome (mm10) using the STAR software (v2.6.1) with default parameters[35] and the GENCODE gene annotation (M23 release).

Differential expression analysis

The R package DESeq2 (v1.35.2) was used to perform differential expression analysis[36], with significant change set to Log2FoldChange > 1 (or < −1) and adjusted P value < 0.05. For overrepresentation analysis (ORA) of significantly differentially expressed genes (DEGs), the "enricher" function from the ClusterProfiler (v4.4.4) package was used with Fisher exact test and default parameters to test enrichment of the DEGs in pathways in the Molecular Signatures Database via the R package msigdbr (v7.5.1)[37,38]. Customized scripts were used to derive gene set clusters and percent of differentially expressed genes using the enrichment maps generated by the emapplot function from ClusterProfiler. Gene

set enrichment analysis (GSEA) of the Hallmarks gene sets from the Molecular signatures database was performed using the fgsea R package, with genes ranked by multiplication of negative natural log-transformed P value and the sign of log fold change[39]. Principal component analysis was performed after transforming counts via the “rlog” R function from DESeq2, taking the top 2000 most highly variable genes, and using the “prcomp” function in R.

Deconvolution analysis of mouse bulk RNA-seq data

For deconvolution of the TKO and DKO bulk RNA-seq tumor data, the R package mouse Microenvironment Cell Population Counter (mMCP-Counter) was used[40]. Infiltration was compared in TKO vs DKO via two-sample t-test. To analyze cytokine expression, we used a cytokine panel derived from the signature “KEGG CYTOKINE-CYTOKINE RECEPTOR INTERACTION” downloaded via msigdbr and removed any receptor genes in the panel. Then, we selected for only differentially expressed cytokines for presentation.

Macrophage polarization analysis

To study macrophage polarization in the TKO bulk RNA-seq data, we downloaded single-cell RNA-seq data of macrophage polarization states[41]. We performed integration, batch correction, and marker analysis of M0, M1, and M2 states using the R package RISC[42]. Using these markers, we performed a Fisher exact test in R to test if markers of each state were enriched in the TKO upregulated genes.

Immunohistochemical staining

Mouse limb tumor tissues were harvested and fixed with 10% formalin, then underwent decalcification with OSTEOSOFT mild decalcifier-solution for histology (Millipore, #101728) for 24 hours or longer until penetrable with a syringe needle. The tissues were re-fixed with formalin then embedded in paraffin wax and sectioned with 5μm thickness. Slides were deparaffinized, hydrated, treated with 3% H2O2 to block endogenous peroxidase then incubated in a steamer for 30 minutes in Target Retrieval Solution (Dako, #S1699, #S2367) for antigen retrieval. Sections were treated with Protein Block (Dako, #X090930–2) then incubated with primary F4/80 (Cell Signaling Technology, #70076), Iba-1 (Abcam, #ab178846), or CD31 (Abcam, #ab28364) antibodies at 4°C overnight. On the next day slides were washed, then incubated with secondary antibody (Cell Signaling Technology, #8114S) for 30 minutes. DAB Substrate Kit (Cell Marque, #957D-20) and Hematoxylin (Fisher HealthCare, #220–101) were used for staining and counterstaining. Slides were visualized with EVOS FL Auto Imaging System (AMC1000, ThermoFisher), or scanned with P250 High Capacity Slide Scanner (3DHISTECH) and viewed with CaseViewer (v2.4, 3DHISTECH). For staining quantification, tumor areas were mapped using QuPath (v0.3.2) as regions of interest (ROIs), then the ROIs underwent cell detection and positive staining detection under same parameters across all slides to get the total number of cells, total number and percentage of positively stained cells. To measure intratumoral microvessel density (iMVD), all vessels were counted in neovascular “hotspot” at 200x magnification in CD31 stained slides, and scored as 1–5 where 1(1–25), 2(256–50), 3(51–100), 4(101–150) and 5(150+)[43,44]. GraphPad Prism 9.0 was used to analyze the results. To test the hypothesis of more macrophage infiltration into TKO tumors, a one-sided two-sample t-test was used

to compare positive cell percentage in TKO vs DKO samples. To test the hypothesis of increased iMVD in TKO, a one-sided two-sample Wilcoxon test was used.

Quantitative PCR analysis

Total RNA was isolated using the RNAeasy Mini Kit (Qiagen) and reverse transcription of total RNA was performed with SuperScript™ IV One-Step RT-PCR System (Thermo Fisher Scientific). Quantitative PCR was performed using the SYBR Green PCR Master Mix (Thermo Fisher Scientific), as previously described[12]. GAPDH was used as the internal control. GraphPad Prism 9.0 was used to analyze the results. PCR primers for *Adgre1* (F4/80) were: (F: ATTGCGGGATTCCTACACTATC; R: TTCACCACCTTCAGGTTTCTC). PCR primers for *Aif1* (Iba-1) were: (F: CCCACCTAGAGCTGAAGAGATTA, R: GATCTCTTGCCCAGCATCATT). To test the hypothesis of more macrophage infiltration into TKO tumors, a one-sided t-test was used to compare expression of macrophage markers in TKO vs DKO samples.

Transcriptomic and survival analysis in clinical cohorts of OS and other cancers

We downloaded clinical and transcriptomic data from the NCI TARGET OS cohort using the TARGET data portal[45,46], and clinical and transcriptomic data from the Kuijjer 2012 cohort using the R2 genomics portal (accession “Kuijjer - 127 - vst - ilmnhwg6v2”)[47]. We filtered the data to keep only patients with both RNA-seq and survival data and no abnormally low TPM values, leading to 83 patients for the NCI TARGET OS and 84 for the Kuijjer cohort. To find homologs between mouse and human genes, we used the R package biomaRt[48]. To calculate expression scores for the TKO overexpressed genes, we used the module score method, which bins genes by their expression level, selects random genes from similar expression bins, calculates means of test and random genes, and subtracts to obtain the difference[49]. To calculate the “TKO myeloid only” signature, we used the MSIGDB C8 cell signature category downloaded via msigdbr and searched for all gene sets with the term “myeloid” in the title, then took the intersect of the genes in these sets with the significantly upregulated TKO genes. For deconvolution analysis of the NCI TARGET OS and Kuijjer 2012 cohort RNA-seq data, we used Microenvironment Cell Population Counter (MCP-Counter), the human counterpart of the mouse-focused mMCP-Counter[50].

For survival analysis with the module scores and MCP counter infiltration scores, we used the survival (v3.4.0) and survminer (v0.4.9) packages in R for both Kaplan-Meier (KM) and Cox regression analysis. For KM we dichotomized the module scores or MCP-Counter scores at the median value to compare survival in high versus low with plots with KM and log-rank tests. For Cox regression, we input the scores as univariate continuous, dichotomized, and tercile analysis. Additionally, we performed the survival analysis on all clinical variables available in the NCI-TARGET data, including age, sex, and presence of metastases at diagnosis. We performed multivariable Cox regression for each module score and MCP-Counter using the only such clinical variable that was significantly associated with survival (metastasis at diagnosis). Finally, we assessed the assumption of proportional hazards for each Cox regression model via graphical and statistical tests of Schoenfield residuals using the “ggcoxzph” and “cox.zph” functions and observed no deviations.

To test SKP2 correlations with other genes and with MCP-Counter immune infiltration scores, we used Pearson correlation with the cor.test function in R. For correlation analysis of all other genes, we also used multiple test correction with the false discovery rate (FDR) method and defined significant correlation as those with FDR < 0.05. We used Fisher exact tests to test for overlap of the TKO gene signature with the negatively correlated genes. For TCGA analysis we downloaded data directly from the Genomic Data Commons website using the TCGABiolinks R package[51]. We used the cor.test function to test the correlation of SKP2 with MCP counter monocyte lineage score. We also used the Timer2.0 web portal to study the correlation of SKP2 expression and survival with monocyte and macrophage infiltration scores[52].

Data Availability Statement

The data generated in this study are publicly available in the Gene Expression Omnibus (GEO) (accession number: GSE226634).

Results

SKP2-KO induces overexpression of immune related genes

We recently developed a transgenic OS mouse model with germline *Skp2* knockout ("TKO": Osx1-Cre;Rb1$^{lox/lox}$;p53$^{lox/lox}$;SKP2) and compared it to a baseline model ("DKO": Osx1-Cre;Rb1$^{lox/lox}$;p53$^{lox/lox}$)[11] for their pre-clinical pathologic features [53]. The result showed that TKO mice experience improved survival compared to DKO mice, with delayed detectable tumorigenesis, slower tumor growth, increased apoptosis, and reduced stemness in TKO tumors.

To study the transcriptional effects of SKP2, we performed RNA-seq on OS tumors (n=3) from both models [Fig 1A]. We detected thousands of genes significantly differentially expressed with > 2 fold changes and at the adjusted p-value < 0.05 (1,736 genes significantly upregulated, 940 downregulated) [Fig 1B]. SKP2 expression was confirmed to be completely abolished in the TKO samples [Supplementary table 2]. Surprisingly, many of the top genes overexpressed in the TKO were related to microenvironment signatures, especially immune-related genes including complement factors such as *C1qa* and major histocompatibility complex class 2 (MHC2) component *H2-Aa*. Gene set overrepresentation analysis showed that TKO tumors upregulated gene signatures related to immune function, muscle- and actin-related genes, endothelial function, and KRAS signaling [Fig 1C, E]. Concordant with these, we observed significant upregulation in TKO of pan-immune marker *Ptprc* (CD45) and endothelial marker *Pecam1*, and modest upregulation of *Kras* [Supplementary table 2]. To infer what transcriptional networks and their top regulators are impacted in TKO tumors, we next analyzed enrichment of transcription factor targets and cancer-related pathway genes. Analysis of transcription factor target signatures from MSIGDB revealed upregulation of MEF2A targets, CBFA2T2 and CBFA2T3 targets, TCF3 targets, and TFAP4 targets, among others [Fig 1E, middle panel, Supplementary Figure 1A]. Additionally, we checked the enrichment of MSIGDB oncogenic signatures in the TKO upregulated genes [Fig 1E lower panel, Supplementary figure 1C]. We found significant enrichment of "SNF5_DN.V1_UP", genes upregulated in *SNF5* knockout (also known as

Smarcb1 or *Baf47*), which was consistent with downregulation of SNF5 targets in TKO. Furthermore, we observed upregulation of *MEK1* (*Map2k1*) and *Kras* targets.

Conversely, gene sets enriched among downregulated genes in TKO relative to DKO were dominated by signatures of hypoxia, along with lipid metabolism and EMT/invasiveness [Fig 1D, F]. Accordingly, we observed significant downregulation of hypoxia response factors Hif1a and vascular endothelial growth factor ligands Vegfa and Vegfd, cholesterol synthesis enzymes including Sqle and Fdft1, and extracellular matrix remodeling proteins such as Mmp3 and Try5 [Supplementary table 2]. Transcription factor activity downregulated by TKO included PRDM4 targets, many of the C/EBP family targets including C/EBPD and CHOP targets, and NF-KB targets [Fig 1F, middle panel, Supplementary figure 1B]. Analysis of oncogenic signatures downregulated in TKO detected downregulation of the signature “E2F1_UP.V1_DN”, corresponding to genes downregulated after overexpression of *E2f1*. This is consistent with upregulation of E2f1 targets in TKO. Additionally, we observed downregulation of mTOR and EGFR signatures [Fig 1F, lower panel, Supplementary figure 1D].

Gene set enrichment analysis also indicated that unfolded protein response was significantly downregulated in TKO, while interferon-γ response gene set was upregulated [Supplementary figures 2] (see Discussion).

Taken together, the RNA-seq results suggest a critical shift of the tumor immune microenvironment in the TKO OS and link a set of critical downstream TFs and signaling that may mediate SKP2’s important roles in OS tumor development and progression.

Deconvolution analysis reveals immune and stromal infiltration is enhanced in the TKO tumor microenvironment

The most parsimonious explanation for the increase in immune and other microenvironment signals in the TKO would be an increase in the infiltration of those cell types into the TKO microenvironment. Prior work on immune microenvironment gene expression in OS showed that immune-related gene expression was indeed driven by infiltrating immune cells, rather than by ectopic expression of immune genes in the malignant OS cells[30].

Thus, we hypothesized that the level of immune cell infiltration would be greater in the TKO than in the DKO. To study this, we used a method of bulk RNA-seq deconvolution analysis called murine Microenvironment Cell Population Counter (mMCP-Counter)[40]. We chose this method because it is the newest such tool designed specifically for mouse tumors, rather than other well-known analogous tools like CIBERSORT, which are designed for humans. Applying it to our bulk RNA-seq samples, we observed that overall microenvironment infiltration levels were higher in the TKO compared to the DKO [Fig 2A]. However, this difference was driven by specific cell types, with the strongest enrichment observed for macrophages [Fig 2B]. Other significant differences included B cells, vessels (lymphatic cells and endothelial cells), T cells broadly and specifically CD8 T cells, and basophils. To corroborate this finding, we examined the expression of canonical markers of these cell types and observed significant differences in most of them [Fig 2C]. Markers of malignant OS cells or osteoclasts, which are bone-resident macrophage-like cells involved in bone

resorption, were not significantly differentially expressed. One of the TKO tumors, however, seemed to express osteoclast and osteoblast markers lower than the others. This was further supported with additional markers from a previous report[54], but the within-group difference is smaller compared to the TKO-DKO difference [Supplementary Figure 3].

Because immune infiltration and activity are often mediated by cytokine expression, we investigated the expression of all cytokine genes and found many significantly differentially expressed [Fig 2D], but unfortunately the result did not provide a clear cue on which cytokines might play an active role in recruiting immune cells to TKO OS. For example, CCL2 is important for macrophage infiltration in many cancers but its expression was reduced in the TKO tumors[55,56]. To address the potential functional impacts of increased macrophages in TKO OS, we also characterized the macrophage polarization status. We reanalyzed a previously published single-cell RNA-sequencing data from unstimulated "M0" macrophages, macrophages stimulated *in vitro* to an "M1" phenotype via exposure to lipopolysaccharides, and macrophages stimulated to "M2" phenotype via exposure to IL4 to define specific marker genes for these polarization states [Supplementary figure 4][57]. We found that genes overexpressed in TKO showed significant enrichments for genes expressed higher in all three states: M0 (65 genes, P = 2.9E-13, Fisher exact test), M1 (130 genes, P = 6.1E-4), M2 (54 genes, P = 4.6E-4) [Supplementary figure 4E]. We further checked M1 and M2 signature genes from previous studies of macrophages in OS and other cancers[58–61] and found three M1 (*Cd86, Il1b, H2-Eb1*) and six M2 (*Mrc1, Maf, Msr1, F13a1, Stab1, Ccl3*) genes were expressed higher in the TKO. Taken together, these results suggest that macrophages in all states exist in the TKO tumors, but their ratios are difficult to estimate.

Immune markers detected by RNA-seq are expressed higher in SKP2 KO tumors at the RNA and protein levels

We next used two independent assays to validate our RNA-seq findings of increased immune cell infiltration in TKO tumors. Because macrophages exhibited the greatest difference between TKO and DKO tumors, we focused on confirming their differential abundance. First, we applied quantitative RT-PCR (qPCR) to new tumor samples not included in RNA-sequencing to compare the expression of macrophage marker genes *Adgre1* (F4/80) and *Aif1* (Iba-1). We confirmed that these genes were expressed at a higher level in the TKO tumors relative to DKO (P = 0.042 and P = 0.028, respectively) [Fig 3A, B]. We also observed a high variability in the expression of these markers among the TKO tumors.

Next, we performed quantitative analysis of immunohistochemistry (IHC) staining for the same macrophage markers, *Adgre1* (F4/80) and *Aif1* (Iba-1). In general, we observed more positive cells in the TKO tumors compared to those from DKO [Fig 3C, Supplementary figure 5]. After semi-quantification of positive cell percentages, we found a higher percentage of cells positive for both F4/80 and Iba-1 in TKO relative to DKO tumors (P = 0.035 and P = 0.039, respectively) [Fig 3D, E]. As in the qPCR assays, we observed a high variability in the percentages of F4/80+ and Iba-1+ cells among the TKO tumors. Additionally, we performed IHC staining for endothelial marker CD31 and observed higher intratumoral microvessel density (iMVD) in TKO (P = 0.02) [Supplementary Figure 6].

SKP2 is negatively correlated with macrophage infiltration in OS and other sarcoma patients

To find genes and pathways associated with SKP2 expression in the human OS tumors and how they may be related to macrophage infiltration, we next performed two types of correlation analysis in the National Cancer Institute (NCI)'s TARGET OS cohort[46,62]. First and remarkably, we found that SKP2 expression in the TARGET-OS patients was significantly negatively correlated with macrophage infiltration scores as estimated by MCP-counter [Fig 4A]. This is consistent with our finding of increased macrophages in our *Skp2* KO mouse model (i.e., reduced macrophages in the *Skp2* WT OS). We validated this in a separate cohort of OS patients, in which 84 participants donated pre-treatment biopsy samples for microarray gene expression analysis, downloaded from the R2 genomics database (the "R2 Kuijjer 2012 cohort")[47]; the correlation between *SKP2* expression and monocyte infiltration scores is $r = -0.48$ ($P < 4e\text{-}6$) [Supplementary Figure 7A].

To identify genes that may be regulated by SKP2 in patient OS tumors, we searched for genes whose expression is significantly correlated with *SKP2* expression in the NCI-TARGET OS cohort. We identified hundreds of genes significantly correlated with *SKP2* [Supplementary table 3]. The positively correlated genes were enriched in pathways related to cancer progression, mRNA processing, and cell proliferation. Strikingly, in the negatively correlated genes, we observed pathway enrichment primarily related to immune function, especially macrophages [Supplementary figure 8 B,D]. Furthermore, we found that the TKO upregulated genes were significantly enriched in the negatively correlated genes (odds ratio = 3.95, $P < 0.001$; Fisher's exact test).

Finally, to test if the correlation between *SKP2* expression and macrophages also exists in other cancer types, we extended our analysis to all the tumor samples in The Cancer Genome Atlas (TCGA). This pan-cancer analysis showed that *SKP2* was significantly and negatively correlated with MCP-Counter macrophage infiltration scores in the TCGA-SARC cohort, which is composed of 260 soft-tissue sarcoma patients [Supplementary Figure 7B], but not other cancers. To strengthen our finding, we expanded our study using the Timer 2.0 software, which applied multiple software to estimate immune cell abundance in the TCGA tumors [Supplementary figure 9][52]. The TCGA Sarcoma cohort consistently showed negative correlations between *SKP2* expression and monocyte/macrophage infiltration scores estimated by multiple methods, as well as consistent survival benefits of macrophage infiltration. Other cancer types also showed some evidence of negative correlation of *SKP2* with monocyte/macrophage infiltration or survival association with infiltration, but the results were less consistent than what was obtained for the TCGA-Sarcoma.

Genes upregulated in SKP2 KO tumors are associated with improved survival in OS patients

We have previously found that TKO mice have significantly improved survival compared to DKO mice[53]. Additionally, we have shown that low expression of *SKP2* was correlated with improved overall survival and metastasis-free survival in two distinct cohorts of OS patients[23]. To test if SKP2-related gene expression is associated with survival in OS patients, we performed survival analysis of the NCI TARGET OS cohort[46,62].

We hypothesized that patients highly expressing genes that were upregulated in the TKO samples would exhibit improved survival over patients with lower expression of those genes. After converting the mouse genes to their human homologs, we calculated a module score for all the genes that were either significantly up-regulated or down-regulated in the TKO samples, to obtain a score for the up- and a score for the down-genes for each patient. We observed a significantly improved 5-year overall survival in OS patients with high expression of the TKO upregulated genes, compared to the patients with low expression of the same genes [Fig 4B]. Since many of the up-regulated genes are immune related, we next investigated if the signal was driven by immune signatures. Using the Molecular Signatures Database (MSIGDB)[63], we selected gene sets related to myeloid cell types from the "C8" cell type marker category, and then took the genes in those sets that were upregulated in the TKO. When we tested this TKO-upregulated myeloid immune signature, we found an even stronger survival benefit [Fig 4C]. Independently, we performed deconvolution analysis in the NCI TARGET data using Microenvironment Cell Population Counter (MCP-counter), the human counterpart of the mouse-specific mMCP-Counter method, then tested the survival association of infiltrating immune cell abundance[64]. High MCP infiltration scores for macrophages and CD8+ T cells were significantly associated with improved survival [Fig 4D, 4E]. Additionally, to account for potential confounding factors, we applied independent multivariable Cox models on the MCP-Counter scores using metastasis at diagnosis as a covariate and confirmed the survival benefits for each score [Supplementary table 4].

We attempted to validate our findings in the R2 Kuijjer 2012 cohort and found modest but consistent associations with improved metastasis-free survival for the TKO signature and MCP macrophage and T cell infiltration scores [Supplementary figure 7 C-F].

Taken together, these results indicate a positive association with patient survival for the genes upregulated in the SKP2 KO and the association is likely explained by increased macrophage infiltration to the OS microenvironment.

Discussion

We have previously shown that Skp2 knockout drives improved survival and prognosis in pre-clinical models of OS[53]. Here, we show that *Skp2* knockout leads to a dramatic remodeling of the tumor microenvironment. Multiple cell types including macrophages, T cells, B cells, and vascular cells preferentially infiltrate into the *Skp2*-KO tumors, compared to the *Skp2*-intact tumors. To our knowledge, no prior connection of SKP2 with any solid tumor malignancy tumor microenvironment has been reported, and this is the first high throughput transcriptomic analysis performed in the context of *Skp2* knockout.

We demonstrated that high expression of the genes upregulated in the mouse *Skp2*-KO OS tumors was correlated with improved survival in OS patients. This seems to be explained by greater expression of macrophage-related signature genes in the *SKP2* KO tumors. This is consistent with a previous report of the positive impact of macrophages on prognosis in OS[30]. Strikingly, we discovered a consistent negative correlation between *SKP2* expression and macrophage infiltration in patient cohorts of OS and other cancer types

including soft-tissue sarcomas, suggesting that regulation of the tumor microenvironment could be a key function of SKP2 that extends beyond pre-clinical mouse models. This is especially relevant in the context of recent reports indicating that antibody-based blockade of immunomodulatory signals Cd47 and Gd2 drove macrophage-mediated anti-tumor cytotoxicity via phagocytosis in OS[31]. Additionally, another recent study also indicated that inhibition of L-amino acid transporter 2 (LAT2) enhanced anti-tumor macrophage immunity and sensitized OS to chemotherapy[32]. Taken together, these studies provide a rationale for testing potent future combination therapy strategies in OS that aim to promote immune recruitment via SKP2 inhibition and promote macrophage activation via anti-CD47/GD2 or anti-LAT2 therapeutics.

The knockout of *Skp2* in OS tumors induced a system-wide gene expression response. We detected differential expression of thousands of genes, among which are cytokines, transcription factors, and known cancer-associated genes which may explain our observations. Many of these factors are critical to the regulation of cell proliferation, cell differentiation, and immunity. Therefore, their disruptions may help explain both the improved survival and enhanced immune infiltration in SKP2 KO tumors, but also help uncover the resistance mechanism employed by OS to SKP2 modulation. Several of the transcription factors upregulated upon *Skp2* KO have previously been reported as proteolytic targets of SCF^{SKP2} ubiquitination, such as *TCF3* or Mef2 family members *MEF2C* and *MEF2D*[65,66]. We also observed evidence for *E2F1* upregulation upon *Skp2* KO, which was a major effector of apoptosis upon *Skp2* knockout in the context of RB1/P53 deficiency[16]. Furthermore, we observed downregulation of PI3K/mTOR/AKT pathway targets upon *Skp2* knockout, consistent with SKP2's reported role of stabilizing AKT1 via protective K63 ubiquitination[67].

In addition to such SKP2 targets reported in literature, we also observed significant differential expression of the targets of other transcription factors for which no link with SKP2 has been reported to our knowledge, including upregulation of targets of the paralogs CBFA2T2, CBFA2T3 along with TFAP4, and downregulation of PRDM4 targets. Interestingly, TFAP4 was reported to undergo proteolytic ubiquitination via a different F-box protein related to SKP2 called BTRCP in conjunction with the SCF E3 ligase complex[68]. We also observed downregulation of targets of various CCAAT-enhancer-binding proteins (C/EBP) family members including *C/EBP-B*, *C/EBP-D*, and *CHOP*, as well as *NF-KB*. *NF-KB* and one C/EBP paralog, *C/EBP-A*, were reported to be inhibited by SKP2 and thus many of their targets would be expected to increase expression in the *Skp2* KO tumors; however, we found that these were actually decreased in TKO[69,70].

Paradoxically, many genes involved in growth factor signal transduction were differentially expressed in a discordant manner, including upregulation of KRAS and MEK1 (Map2k1) targets and downregulation of EGFR in *Skp2* KO tumors. It is possible that previously described regulatory relationships may be altered *in vivo* in the context of Rb1/P53 doubly deficient OS. Ultimately, the interaction among different signals and pathways will need more studies in the future to fully understand the benefits and caveats of targeting SKP2.

The mechanism underlying our observations of increased macrophage infiltration remains elusive, but there are several possibilities. Firstly, this may be related to the downregulation of the regulatory targets of CHOP and the unfolded protein response (UPR). UPR is a cellular response to proteotoxic endoplasmic reticulum stress, but it has recently been linked to immunosuppression in cancer, as ablation of UPR unleashed effective anti-tumor immunity via mitochondrial stress followed by activation of STING and interferon signaling[71–73]. Consistent with this, we observed significant upregulation of interferon-response genes in TKO tumors. Secondly, we observed an increase in the intra-tumor microvasculature in TKO tumors, which may lead to an increased accessibility for infiltration of immune cells. Thirdly, germline *Skp2* knockout may exert an effect on hematopoietic populations in general, as SKP2's role in the regulation of hematopoiesis was previously studied. Two reports showed that *Skp2* germline KO led to increased hematopoietic stem cell numbers, but reported opposite results for the effect on the granulocyte/monocyte progenitor population [74,75]. Neither specifically looked at mature monocytes or macrophages. These mechanisms may not be mutually exclusive, and further studies will be required to elucidate which of these, if any, explains the phenotypes we have observed.

There are limitations in the current study. One is that the technical nature of bulk RNA-seq does not allow direct profiling of the gene expression in individual cellular components. This may have limited our ability to address if the OS malignant cells directly promote the recruitment of macrophages to tumors, for example, our comparison of cytokine analysis was based on the cytokines produced by all cell types. New methods like single-cell RNA-sequencing or spatial transcriptomics will allow more precise study of the effects of *Skp2* KO in distinct populations of malignant cells and TME compartments. Additionally, it is unclear if SKP2 exerts the described microenvironment-remodeling effect within malignant cells, infiltrating immune cells, or both, due to the organism-wide nature of the germline *Skp2* knockout. While this model does reflect the clinical setting of system-wide SKP2 inhibition, a secondary model of conditional *Skp2*-KO via OSX-Cre lox would allow us to study the SKP2-monocyte recruitment mechanism in more detail. Lastly, considering the genetic diversity of OS and the variability of our models, additional samples would help strengthen our results.

Supplementary Material

Refer to Web version on PubMed Central for supplementary material.

Acknowledgements

This study is supported by the National Institutes of Health (NIH/NCI) (R01CA255643 to B.H.) and Sarcoma Strong (to B.H.). A.F. is supported by the PhD in Clinical Investigation program at Albert Einstein College of Medicine under NIH/National Center for Advancing Translational Science (NCATS) Einstein-Montefiore CTSA Grant Number (UL1TR001073) and NIH TG number (TL1TR0022557). J.W. would like to acknowledge the supports of National Natural Science Foundation of China (82103223 to J.W.), Peking University Peoplès Hospital Scientific Research Development Funds (RDX2022-01 to J.W.), and Peking University Clinical Scientist Training Program (BMU2023PYJH015 to J.W.).

References

1. Sissons HA. The WHO classification of bone tumors. Recent Results in Cancer Research. 1976;Vol. 54:104–108. doi:10.1007/978-3-642-80997-2_8
2. Prater S, McKeon B. Cancer, Osteosarcoma. StatPearls Publishing; 2019.
3. Mirabello L, Troisi RJ, Savage SA. Osteosarcoma incidence and survival rates from 1973 to 2004: Data from the surveillance, epidemiology, and end results program. Cancer. 2009;115(7):1531–1543. doi:10.1002/cncr.24121 [PubMed: 19197972]
4. Bielack SS, Kempf-Bielack B, Delling G, Exner GU, Flege S, Helmke K, Kotz R, Salzer-Kuntschik M, Werner M, Winkelmann W, Zoubek A, Jürgens H, Winkler K. Prognostic Factors in High-Grade Osteosarcoma of the Extremities or Trunk: An Analysis of 1,702 Patients Treated on Neoadjuvant Cooperative Osteosarcoma Study Group Protocols. Journal of Clinical Oncology. 2002;20(3):776–790. doi:10.1200/jco.2002.20.3.776 [PubMed: 11821461]
5. Kaste SC, Pratt CB, Cain AM, Jones-Wallace DJ, Rao BN. Metastases detected at the time of diagnosis of primary pediatric extremity osteosarcoma at diagnosis: Imaging features. Cancer. 1999;86(8):1602–1608. doi:10.1002/(SICI)1097-0142(19991015)86:8<1602::AID-CNCR31>3.0.CO;2-R [PubMed: 10526292]
6. Chen X, Bahrami A, Pappo A, Easton J, Dalton J, Hedlund E, Ellison D, Shurtleff S, Wu G, Wei L, Parker M, Rusch M, Nagahawatte P, Wu J, Mao S, Boggs K, Mulder H, Yergeau D, Lu C, Ding L, Edmonson M, Qu C, Wang J, Li Y, Navid F, Daw NC, Mardis ER, Wilson RK, Downing JR, Zhang J, Dyer MA. Recurrent somatic structural variations contribute to tumorigenesis in pediatric osteosarcoma. Cell Reports. 2014;7(1):104–112. doi:10.1016/j.celrep.2014.03.003 [PubMed: 24703847]
7. Perry JA, Kiezun A, Tonzi P, Van Allen EM, Carter SL, Baca SC, Cowley GS, Bhatt AS, Rheinbay E, Pedamallu CS, Helman E, Taylor-Weiner A, McKenna A, DeLuca DS, Lawrence MS, Ambrogio L, Sougnez C, Sivachenko A, Walensky LD, Wagle N, Mora J, De Torres C, Lavarino C, Dos Santos Aguiar S, Yunes JA, Brandalise SR, Mercado-Celis GE, Melendez-Zajgla J, Cárdenas-Cardós R, Velasco-Hidalgo L, Roberts CWM, Garraway LA, Rodriguez-Galindo C, Gabriel SB, Lander ES, Golub TR, Orkin SH, Getz G, Janeway KA. Complementary genomic approaches highlight the PI3K/mTOR pathway as a common vulnerability in osteosarcoma. Proceedings of the National Academy of Sciences of the United States of America. 2014;111(51):E5564–E5573. doi:10.1073/pnas.1419260111 [PubMed: 25512523]
8. Wang D, Niu X, Wang Z, Song CL, Huang Z, Chen KN, Duan J, Bai H, Xu J, Zhao J, Wang Y, Zhuo M, Sunney Xie X, Kang X, Tian Y, Cai L, Han JF, An T, Sun Y, Gao S, Zhao J, Ying J, Wang L, He J, Wang J. Multiregion sequencing reveals the genetic heterogeneity and evolutionary history of osteosarcoma and matched pulmonary metastases. Cancer Research. 2019;79(1):7–20. doi:10.1158/0008-5472.CAN-18-1086 [PubMed: 30389703]
9. Martin JW, Squire JA, Zielenska M. The genetics of osteosarcoma. Sarcoma. 2012;2012. doi:10.1155/2012/627254
10. Morrow JJ, Khanna C. Osteosarcoma genetics and epigenetics: Emerging biology and candidate therapies. Critical Reviews in Oncogenesis. 2015;20(3–4):173–197. doi:10.1615/CritRevOncog.2015013713 [PubMed: 26349415]
11. Walkley CR, Qudsi R, Sankaran VG, Perry JA, Gostissa M, Roth SI, Rodda SJ, Snay E, Dunning P, Fahey FH, Alt FW, McMahon AP, Orkin SH. Conditional mouse osteosarcoma, dependent on p53 loss and potentiated by loss of Rb, mimics the human disease. Genes and Development. 2008;22(12):1662–1676. doi:10.1101/gad.1656808 [PubMed: 18559481]
12. Wang J, Aldahamsheh O, Ferrena A, Borjihan H, Singla A, Yaguare S, Singh S, Viscarret V, Tingling J, Zi X, Lo Y, Gorlick R, Zheng D, Schwartz EL, Zhao H, Yang R, Geller DS, Hoang BH. The interaction of SKP2 with p27 enhances the progression and stemness of osteosarcoma. Annals of the New York Academy of Sciences. February 2021. doi:10.1111/nyas.14578
13. Asmamaw MD, Liu Y, Zheng Y, Shi X, Liu H. Skp2 in the ubiquitin-proteasome system: A comprehensive review. Medicinal Research Reviews. 2020;40(5):1920–1949. doi:10.1002/med.21675 [PubMed: 32391596]

14. Kossatz U, Dietrich N, Zender L, Buer J, Manns MP, Malek NP. Skp2-dependent degradation of p27kip1 is essential for cell cycle progression. Genes and Development. 2004;18(21):2602–2607. doi:10.1101/gad.321004 [PubMed: 15520280]
15. Wang W, Nacusi L, Sheaff RJ, Liu X. Ubiquitination of p21Cip1/WAF1 by SCFSkp2: Substrate requirement and ubiquitination site selection. Biochemistry. 2005;44(44):14553–14564. doi:10.1021/bi051071j [PubMed: 16262255]
16. Zhao H, Bauzon F, Fu H, Lu Z, Cui J, Nakayama K, Nakayama KI, Locker J, Zhu L. Skp2 Deletion Unmasks a p27 Safeguard that Blocks Tumorigenesis in the Absence of pRb and p53 Tumor Suppressors. Cancer Cell. 2013;24(5):645–659. doi:10.1016/j.ccr.2013.09.021 [PubMed: 24229711]
17. Wang H, Bauzon F, Ji P, Xu X, Sun D, Locker J, Sellers RS, Nakayama K, Nakayama KI, Cobrinik D, Zhu L. Skp2 is required for survival of aberrantly proliferating Rb1-deficient cells and for tumorigenesis in Rb1+/− mice. Nature genetics. 2010;42(1):83–88. doi:10.1038/NG.498 [PubMed: 19966802]
18. Zhao H, Wang H, Bauzon F, Lu Z, Fu H, Cui J, Zhu L. Deletions of Retinoblastoma 1 (Rb1) and Its Repressing Target S Phase Kinase-associated protein 2 (Skp2) Are Synthetic Lethal in Mouse Embryogenesis. The Journal of biological chemistry. 2016;291(19):10201–10209. doi:10.1074/JBC.M116.718049 [PubMed: 26966181]
19. Old JB, Kratzat S, Hoellein A, Graf S, Nilsson JA, Nilsson L, Nakayama KI, Peschel C, Cleveland JL, Keller UB. Skp2 directs Myc-mediated suppression of p27Kip1 yet has modest effects on Myc-driven lymphomagenesis. Molecular cancer research : MCR. 2010;8(3):353. doi:10.1158/1541-7786.MCR-09-0232 [PubMed: 20197382]
20. Soucy TA, Smith PG, Milhollen MA, Berger AJ, Gavin JM, Adhikari S, Brownell JE, Burke KE, Cardin DP, Critchley S, Cullis CA, Doucette A, Garnsey JJ, Gaulin JL, Gershman RE, Lublinsky AR, McDonald A, Mizutani H, Narayanan U, Olhava EJ, Peluso S, Rezaei M, Sintchak MD, Talreja T, Thomas MP, Traore T, Vyskocil S, Weatherhead GS, Yu J, Zhang J, Dick LR, Claiborne CF, Rolfe M, Bolen JB, Langston SP. An inhibitor of NEDD8-activating enzyme as a new approach to treat cancer. Nature. 2009;458(7239):732–736. doi:10.1038/nature07884 [PubMed: 19360080]
21. Wu L, Grigoryan AV., Li Y, Hao B, Pagano M, Cardozo TJ. Specific small molecule inhibitors of skp2-mediated p27 degradation. Chemistry and Biology. 2012;19(12):1515–1524. doi:10.1016/j.chembiol.2012.09.015 [PubMed: 23261596]
22. Chan CH, Morrow JK, Li CF, Gao Y, Jin G, Moten A, Stagg LJ, Ladbury JE, Cai Z, Xu D, Logothetis CJ, Hung MC, Zhang S, Lin HK. Pharmacological inactivation of Skp2 SCF ubiquitin ligase restricts cancer stem cell traits and cancer progression. Cell. 2013;154(3). doi:10.1016/J.CELL.2013.06.048
23. Zhang Y, Zvi YS, Batko B, Zaphiros N, O'Donnell EF, Wang J, Sato K, Yang R, Geller DS, Koirala P, Zhang W, Du X, Piperdi S, Liu Y, Zheng D, Roth M, Gill J, Zhang J, Ren T, Gorlick R, Zi X, Hoang BH. Down-regulation of Skp2 expression inhibits invasion and lung metastasis in osteosarcoma. Scientific Reports. 2018;8(1). doi:10.1038/s41598-018-32428-9
24. Wang J, Ferrena A, Singh S, Viscarret V, Al-Hardan W, Aldahamsheh O, Borjihan H, Singla A, Yaguare S, Tingling J, Zi X, Lo Y, Gorlick R, Schwartz EL, Zhao H, Yang R, Geller DS, Zheng D, Hoang BH. Targeted inhibition of SCF-SKP2 confers anti-tumor activities resulting in a survival benefit in osteosarcoma. bioRxiv. May 2023:2023.05.13.540637. doi:10.1101/2023.05.13.540637
25. Zhou Y, Yang D, Yang Q, Lv X, Huang W, Zhou Z, Wang Y, Zhang Z, Yuan T, Ding X, Tang L, Zhang J, Yin J, Huang Y, Yu W, Wang Y, Zhou C, Su Y, He A, Sun Y, Shen Z, Qian B, Meng W, Fei J, Yao Y, Pan X, Chen P, Hu H. Single-cell RNA landscape of intratumoral heterogeneity and immunosuppressive microenvironment in advanced osteosarcoma. Nature Communications. 2020;11(1):1–17. doi:10.1038/s41467-020-20059-6
26. Liu Y, Feng W, Dai Y, Bao M, Yuan Z, He M, Qin Z, Liao S, He J, Huang Q, Yu Z, Zeng Y, Guo B, Huang R, Yang R, Jiang Y, Liao J, Xiao Z, Zhan X, Lin C, Xu J, Ye Y, Ma J, Wei Q, Mo Z. Single-Cell Transcriptomics Reveals the Complexity of the Tumor Microenvironment of Treatment-Naive Osteosarcoma. Frontiers in Oncology. 2021;11:2818. doi:10.3389/FONC.2021.709210/BIBTEX
27. Wu CC, Beird HC, Andrew Livingston J, Advani S, Mitra A, Cao S, Reuben A, Ingram D, Wang WL, Ju Z, Hong Leung C, Lin H, Zheng Y, Roszik J, Wang W, Patel S, Benjamin RS,

Somaiah N, Conley AP, Mills GB, Hwu P, Gorlick R, Lazar A, Daw NC, Lewis V, Futreal PA. Immuno-genomic landscape of osteosarcoma. Nature Communications. 2020;11(1):1–11. doi:10.1038/s41467-020-14646-w

28. Tawbi HA, Burgess M, Bolejack V, van Tine BA, Schuetze SM, Hu J, D'Angelo S, Attia S, Riedel RF, Priebat DA, Movva S, Davis LE, Okuno SH, Reed DR, Crowley J, Butterfield LH, Salazar R, Rodriguez-Canales J, Lazar AJ, Wistuba II, Baker LH, Maki RG, Reinke D, Patel S. Pembrolizumab in advanced soft-tissue sarcoma and bone sarcoma (SARC028): a multicentre, two-cohort, single-arm, open-label, phase 2 trial. The Lancet Oncology. 2017;18(11):1493–1501. doi:10.1016/S1470-2045(17)30624-1 [PubMed: 28988646]
29. D'Angelo SP, Mahoney MR, van Tine BA, Atkins J, Milhem MM, Jahagirdar BN, Antonescu CR, Horvath E, Tap WD, Schwartz GK, Streicher H. Nivolumab with or without ipilimumab treatment for metastatic sarcoma (Alliance A091401): two open-label, non-comparative, randomised, phase 2 trials. The Lancet Oncology. 2018;19(3):416–426. doi:10.1016/S1470-2045(18)30006-8 [PubMed: 29370992]
30. Buddingh EP, Kuijjer ML, Duim RAJ, Bürger H, Agelopoulos K, Myklebost O, Serra M, Mertens F, Hogendoorn PCW, Lankester AC, Cleton-Jansen AM. Tumor-infiltrating macrophages are associated with metastasis suppression in high-grade osteosarcoma: a rationale for treatment with macrophage activating agents. Clinical cancer research : an official journal of the American Association for Cancer Research. 2011;17(8):2110–2119. doi:10.1158/1078-0432.CCR-10-2047 [PubMed: 21372215]
31. Theruvath J, Menard M, Smith BAH, Linde MH, Coles GL, Dalton GN, Wu W, Kiru L, Delaidelli A, Sotillo E, Silberstein JL, Geraghty AC, Banuelos A, Radosevich MT, Dhingra S, Heitzeneder S, Tousley A, Lattin J, Xu P, Huang J, Nasholm N, He A, Kuo TC, Sangalang ERB, Pons J, Barkal A, Brewer RE, Marjon KD, Vilches-Moure JG, Marshall PL, Fernandes R, Monje M, Cochran JR, Sorensen PH, Daldrup-Link HE, Weissman IL, Sage J, Majeti R, Bertozzi CR, Weiss WA, Mackall CL, Majzner RG. Anti-GD2 synergizes with CD47 blockade to mediate tumor eradication. Nature Medicine 2022 28:2. 2022;28(2):333–344. doi:10.1038/s41591-021-01625-x
32. Wang Z, Li B, Li S, Lin W, Wang Z, Wang S, Chen W, Shi W, Chen T, Zhou H, Yinwang E, Zhang W, Mou H, Chai X, Zhang J, Lu Z, Ye Z. Metabolic control of CD47 expression through LAT2-mediated amino acid uptake promotes tumor immune evasion. Nature Communications 2022 13:1. 2022;13(1):1–19. doi:10.1038/s41467-022-34064-4
33. Luo ZW, Liu PP, Wang ZX, Chen CY, Xie H. Macrophages in Osteosarcoma Immune Microenvironment: Implications for Immunotherapy. Frontiers in Oncology. 2020;10. doi:10.3389/FONC.2020.586580 [PubMed: 32047721]
34. Zhao H, Iqbal NJ, Sukrithan V, Nicholas C, Xue Y, Yu C, Locker J, Zou J, Schwartz EL, Zhu L. Targeted Inhibition of the E3 Ligase SCFSkp2/Cks1 Has Antitumor Activity in RB1-Deficient Human and Mouse Small-Cell Lung Cancer. Cancer research. 2020;80(11):2355–2367. doi:10.1158/0008-5472.CAN-19-2400 [PubMed: 32265224]
35. Dobin A, Davis CA, Schlesinger F, Drenkow J, Zaleski C, Jha S, Batut P, Chaisson M, Gingeras TR. STAR: Ultrafast universal RNA-seq aligner. Bioinformatics. 2013;29(1):15–21. doi:10.1093/bioinformatics/bts635 [PubMed: 23104886]
36. Love MI, Huber W, Anders S. Moderated estimation of fold change and dispersion for RNA-seq data with DESeq2. Genome Biology. 2014;15(550):1–21. doi:10.1186/s13059-014-0550-8
37. Dolgalev I msigdbr: MSigDB Gene Sets for Multiple Organisms in a Tidy Data Format. R package version 6.2.1. 2018. https://CRAN.R-project.org/package=msigdbr.
38. Wu T, Hu E, Xu S, Chen M, Guo P, Dai Z, Feng T, Zhou L, Tang W, Zhan L, Fu X, Liu S, Bo X, Yu G. clusterProfiler 4.0: A universal enrichment tool for interpreting omics data. Innovation (Cambridge (Mass)). 2021;2(3). doi:10.1016/J.XINN.2021.100141
39. Korotkevich G, Sukhov V, Budin N, Shpak B, Artyomov MN, Sergushichev A. Fast gene set enrichment analysis. bioRxiv. February 2021:060012. doi:10.1101/060012
40. Petitprez F, Levy S, Sun CM, Meylan M, Linhard C, Becht E, Elarouci N, Tavel D, Roumenina LT, Ayadi M, Sautès-Fridman C, Fridman WH, de Reyniès A. The murine Microenvironment Cell Population counter method to estimate abundance of tissue-infiltrating immune and stromal cell populations in murine samples using gene expression. Genome Medicine. 2020;12(1). doi:10.1186/S13073-020-00783-W

41. Li C, Menoret A, Farragher C, Ouyang Z, Bonin C, Holvoet P, Vella AT, Zhou B. Single cell transcriptomics based-MacSpectrum reveals novel macrophage activation signatures in diseases. JCI insight. 2019;5(10). doi:10.1172/JCI.INSIGHT.126453
42. Liu Y, Wang T, Zhou B, Zheng D. Robust integration of multiple single-cell RNA sequencing datasets using a single reference space. Nature biotechnology. 2021;39(7):877–884. doi:10.1038/S41587-021-00859-X
43. Weidner N Current pathologic methods for measuring intratumoral microvessel density within breast carcinoma and other solid tumors. Breast cancer research and treatment. 1995;36(2):169–180. doi:10.1007/BF00666038 [PubMed: 8534865]
44. Minopoli M, Sarno S, Di Carluccio G, Azzaro R, Costantini S, Fazioli F, Gallo M, Apice G, Cannella L, Rea D, Stoppelli MP, Boraschi D, Budillon A, Scotlandi K, De Chiara A, Carriero MV. Inhibiting Monocyte Recruitment to Prevent the Pro-Tumoral Activity of Tumor-Associated Macrophages in Chondrosarcoma. Cells. 2020;9(4). doi:10.3390/CELLS9041062
45. TARGET Data Matrix | Office of Cancer Genomics. https://ocg.cancer.gov/programs/target/data-matrix. Accessed February 23, 2022.
46. Ma X, Liu Y, Liu Y, Alexandrov LB, Edmonson MN, Gawad C, Zhou X, Li Y, Rusch MC, John E, Huether R, Gonzalez-Pena V, Wilkinson MR, Hermida LC, Davis S, Sioson E, Pounds S, Cao X, Ries RE, Wang Z, Chen X, Dong L, Diskin SJ, Smith MA, Auvi JMG, Meltzer PS, Lau CC, Perlman EJ, Maris JM, Meshinchi S, Hunger SP, Gerhard DS, Zhang J. Pan-cancer genome and transcriptome analyses of 1,699 paediatric leukaemias and solid tumours. Nature 2018 555:7696. 2018;555(7696):371–376. doi:10.1038/nature25795
47. Kuijjer ML, Rydbeck H, Kresse SH, Buddingh EP, Lid AB, Roelofs H, Bürger H, Myklebost O, Hogendoorn PCW, Meza-Zepeda LA, Cleton-Jansen AM. Identification of osteosarcoma driver genes by integrative analysis of copy number and gene expression data. Genes Chromosomes and Cancer. 2012;51(7):696–706. doi:10.1002/gcc.21956 [PubMed: 22454324]
48. Durinck S, Moreau Y, Kasprzyk A, Davis S, de Moor B, Brazma A, Huber W. BioMart and Bioconductor: A powerful link between biological databases and microarray data analysis. Bioinformatics. 2005;21(16):3439–3440. doi:10.1093/bioinformatics/bti525 [PubMed: 16082012]
49. Tirosh I, Izar B, Prakadan SM, Wadsworth MH, Treacy D, Trombetta JJ, Rotem A, Rodman C, Lian C, Murphy G, Fallahi-Sichani M, Dutton-Regester K, Lin JR, Cohen O, Shah P, Lu D, Genshaft AS, Hughes TK, Ziegler CGK, Kazer SW, Gaillard A, Kolb KE, Villani AC, Johannessen CM, Andreev AY, van Allen EM, Bertagnolli M, Sorger PK, Sullivan RJ, Flaherty KT, Frederick DT, Jané-Valbuena J, Yoon CH, Rozenblatt-Rosen O, Shalek AK, Regev A, Garraway LA. Dissecting the multicellular ecosystem of metastatic melanoma by single-cell RNA-seq. Science. 2016;352(6282):189–196. doi:10.1126/science.aad0501 [PubMed: 27124452]
50. Becht E, Giraldo NA, Lacroix L, Buttard B, Elarouci N, Petitprez F, Selves J, Laurent-Puig P, Sautès-Fridman C, Fridman WH, de Reyniès A. Estimating the population abundance of tissue-infiltrating immune and stromal cell populations using gene expression. Genome Biology. 2016;17(1):1–20. doi:10.1186/S13059-016-1070-5/TABLES/4 [PubMed: 26753840]
51. Colaprico A, Silva TC, Olsen C, Garofano L, Cava C, Garolini D, Sabedot TS, Malta TM, Pagnotta SM, Castiglioni I, Ceccarelli M, Bontempi G, Noushmehr H. TCGAbiolinks: an R/Bioconductor package for integrative analysis of TCGA data. Nucleic Acids Research. 2016;44(8):e71–e71. doi:10.1093/NAR/GKV1507 [PubMed: 26704973]
52. Li T, Fu J, Zeng Z, Cohen D, Li J, Chen Q, Li B, Liu XS. TIMER2.0 for analysis of tumor-infiltrating immune cells. Nucleic acids research. 2020;48(W1):W509–W514. doi:10.1093/NAR/GKAA407 [PubMed: 32442275]
53. Wang J, Aldahamsheh O, Ferrena A, Singh S, Singla A, Borjihan H, Yaguare S, Viscarret V, Tingling J, Zi X, Lo Y, Gorlick R, Zheng D, Schwartz EL, Zhao H, Yang R, Geller DS, Hoang BH. Abstract 2008: Targeting SKP2 by p27 Inhibits stemness and prolong the survival in osteosarcoma. Cancer Research. 2021;81(13_Supplement):2008–2008. doi:10.1158/1538-7445.AM2021-2008
54. Dolgalev I, Tikhonova AN. Connecting the Dots: Resolving the Bone Marrow Niche Heterogeneity. Frontiers in Cell and Developmental Biology. 2021;9:622519. doi:10.3389/FCELL.2021.622519/BIBTEX [PubMed: 33777933]

55. Mantovani A, Sica A, Sozzani S, Allavena P, Vecchi A, Locati M. The chemokine system in diverse forms of macrophage activation and polarization. Trends in immunology. 2004;25(12):677–686. doi:10.1016/J.IT.2004.09.015 [PubMed: 15530839]
56. Jin J, Lin J, Xu A, Lou J, Qian C, Li X, Wang Y, Yu W, Tao H. CCL2: An Important Mediator Between Tumor Cells and Host Cells in Tumor Microenvironment. Frontiers in Oncology. 2021;11:2917. doi:10.3389/FONC.2021.722916/BIBTEX
57. Li C, Menoret A, Farragher C, Ouyang Z, Bonin C, Holvoet P, Vella AT, Zhou B. Single cell transcriptomics based-MacSpectrum reveals novel macrophage activation signatures in diseases. JCI insight. 2019;5(10). doi:10.1172/JCI.INSIGHT.126453
58. Liu Y, Feng W, Dai Y, Bao M, Yuan Z, He M, Qin Z, Liao S, He J, Huang Q, Yu Z, Zeng Y, Guo B, Huang R, Yang R, Jiang Y, Liao J, Xiao Z, Zhan X, Lin C, Xu J, Ye Y, Ma J, Wei Q, Mo Z. Single-Cell Transcriptomics Reveals the Complexity of the Tumor Microenvironment of Treatment-Naive Osteosarcoma. Frontiers in Oncology. 2021;11:709210. doi:10.3389/FONC.2021.709210/BIBTEX [PubMed: 34367994]
59. Tekin C, Aberson HL, Bijlsma MF, Spek CA. Early macrophage infiltrates impair pancreatic cancer cell growth by TNF-α secretion. BMC cancer. 2020;20(1). doi:10.1186/S12885-020-07697-1
60. Genin M, Clement F, Fattaccioli A, Raes M, Michiels C. M1 and M2 macrophages derived from THP-1 cells differentially modulate the response of cancer cells to etoposide. BMC Cancer. 2015;15(1):1–14. doi:10.1186/S12885-015-1546-9/FIGURES/10 [PubMed: 25971837]
61. Jayasingam SD, Citartan M, Thang TH, Mat Zin AA, Ang KC, Ch'ng ES. Evaluating the Polarization of Tumor-Associated Macrophages Into M1 and M2 Phenotypes in Human Cancer Tissue: Technicalities and Challenges in Routine Clinical Practice. Frontiers in Oncology. 2020;9:494426. doi:10.3389/FONC.2019.01512/BIBTEX
62. Osteosarcoma. https://ocg.cancer.gov/programs/target/projects/osteosarcoma. Accessed January 25, 2021.
63. Liberzon A, Birger C, Thorvaldsdóttir H, Ghandi M, Mesirov JP, Tamayo P. The Molecular Signatures Database Hallmark Gene Set Collection. Cell Systems. 2015;1:417–425. doi:10.1016/j.cels.2015.12.004 [PubMed: 26771021]
64. Becht E, Giraldo NA, Lacroix L, Buttard B, Elarouci N, Petitprez F, Selves J, Laurent-Puig P, Sautès-Fridman C, Fridman WH, de Reyniès A. Estimating the population abundance of tissue-infiltrating immune and stromal cell populations using gene expression. Genome Biology. 2016;17(1):1–20. doi:10.1186/S13059-016-1070-5/TABLES/4 [PubMed: 26753840]
65. Giorgio E di, Gagliostro E, Clocchiatti A, Brancolini C. The Control Operated by the Cell Cycle Machinery on MEF2 Stability Contributes to the Downregulation of CDKN1A and Entry into S Phase. Molecular and Cellular Biology. 2015;35(9):1633. doi:10.1128/MCB.01461-14 [PubMed: 25733682]
66. Nie L, Xu M, Vladimirova A, Sun XH. Notch-induced E2A ubiquitination and degradation are controlled by MAP kinase activities. The EMBO journal. 2003;22(21):5780–5792. doi:10.1093/EMBOJ/CDG567 [PubMed: 14592976]
67. Chan CH, Li CF, Yang WL, Gao Y, Lee SW, Feng Z, Huang HY, Tsai KKC, Flores LG, Shao Y, Hazle JD, Yu D, Wei W, Sarbassov D, Hung MC, Nakayama KI, Lin HK. The Skp2-SCF E3 Ligase Regulates Akt Ubiquitination, Glycolysis, Herceptin Sensitivity, and Tumorigenesis. Cell. 2012;149(5):1098–1111. doi:10.1016/J.CELL.2012.02.065 [PubMed: 22632973]
68. D'Annibale S, Kim J, Magliozzi R, Low TY, Mohammed S, Heck AJR, Guardavaccaro D. Proteasome-dependent Degradation of Transcription Factor Activating Enhancer-binding Protein 4 (TFAP4) Controls Mitotic Division. The Journal of Biological Chemistry. 2014;289(11):7730. doi:10.1074/JBC.M114.549535 [PubMed: 24500709]
69. Thacker G, Mishra M, Sharma A, Singh AK, Sanyal S, Trivedi AK. CDK2-instigates C/EBPα degradation through SKP2 in Acute myeloid leukemia. Medical oncology (Northwood, London, England). 2021;38(6). doi:10.1007/S12032-021-01523-9
70. Liu K, Zhang L, Zhao Q, Zhao Z, Zhi F, Qin Y, Cui J. SKP2 attenuates NF-κB signaling by mediating IKKβ degradation through autophagy. Journal of Molecular Cell Biology. 2018;10(3):205–215. doi:10.1093/JMCB/MJY012 [PubMed: 29474632]

71. Cao Y, Trillo-Tinoco J, Sierra RA, Anadon C, Dai W, Mohamed E, Cen L, Costich TL, Magliocco A, Marchion D, Klar R, Michel S, Jaschinski F, Reich RR, Mehrotra S, Cubillos-Ruiz JR, Munn DH, Conejo-Garcia JR, Rodriguez PC. ER stress-induced mediator C/EBP homologous protein thwarts effector T cell activity in tumors through T-bet repression. Nature Communications 2019 10:1. 2019;10(1):1–15. doi:10.1038/s41467-019-09263-1

72. Mohamed E, Sierra RA, Trillo-Tinoco J, Cao Y, Innamarato P, Payne KK, de Mingo Pulido A, Mandula J, Zhang S, Thevenot P, Biswas S, Abdalla SK, Costich TL, Hänggi K, Anadon CM, Flores ER, Haura EB, Mehrotra S, Pilon-Thomas S, Ruffell B, Munn DH, Cubillos-Ruiz JR, Conejo-Garcia JR, Rodriguez PC. The Unfolded Protein Response Mediator PERK Governs Myeloid Cell-Driven Immunosuppression in Tumors through Inhibition of STING Signaling. Immunity. 2020;52(4):668–682.e7. doi:10.1016/J.IMMUNI.2020.03.004 [PubMed: 32294407]

73. Mandula JK, Chang S, Mohamed E, Jimenez R, Sierra-Mondragon RA, Chang DC, Obermayer AN, Moran-Segura CM, Das S, Vazquez-Martinez JA, Prieto K, Chen A, Smalley KSM, Czerniecki B, Forsyth P, Koya RC, Ruffell B, Cubillos-Ruiz JR, Munn DH, Shaw TI, Conejo-Garcia JR, Rodriguez PC. Ablation of the endoplasmic reticulum stress kinase PERK induces paraptosis and type I interferon to promote anti-tumor T cell responses. Cancer Cell. 2022;40(10):1145–1160.e9. doi:10.1016/j.ccell.2022.08.016 [PubMed: 36150390]

74. Rodriguez S, Wang L, Mumaw C, Srour EF, Lo Celso C, Nakayama KI, Carlesso N. The SKP2 E3 ligase regulates basal homeostasis and stress-induced regeneration of HSCs. Blood. 2011;117(24):6509. doi:10.1182/BLOOD-2010-11-321521 [PubMed: 21502543]

75. Wang J, Han F, Wu J, Lee SW, Chan CH, Wu CY, Yang WL, Gao Y, Zhang X, Jeong YS, Moten A, Samaniego F, Huang P, Liu Q, Zeng YX, Lin HK. The role of Skp2 in hematopoietic stem cell quiescence, pool size, and self-renewal. Blood. 2011;118(20):5429. doi:10.1182/BLOOD-2010-10-312785 [PubMed: 21931116]

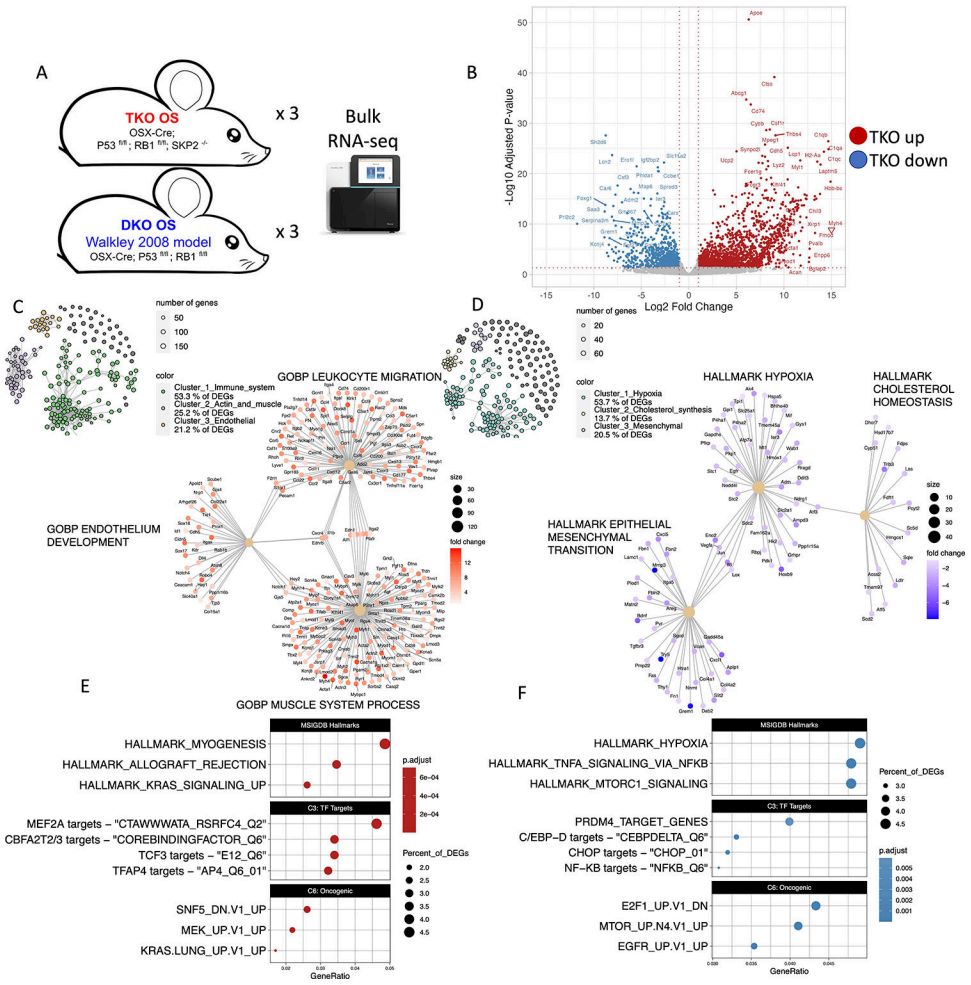

Figure 1: Differential RNA expression analysis.

A): Experimental workflow. **B**): Volcano plot summarizing differential expression between TKO and DKO samples. **C,D**): Network-based gene set overrepresentation analysis of genes upregulated (C) or downregulated (D) in TKO. **E,F**): Dotplots for enrichment of MSIGDB Hallmarks and transcription factor targets, and oncogenic signals upregulated (E) or downregulated (F) in TKO.

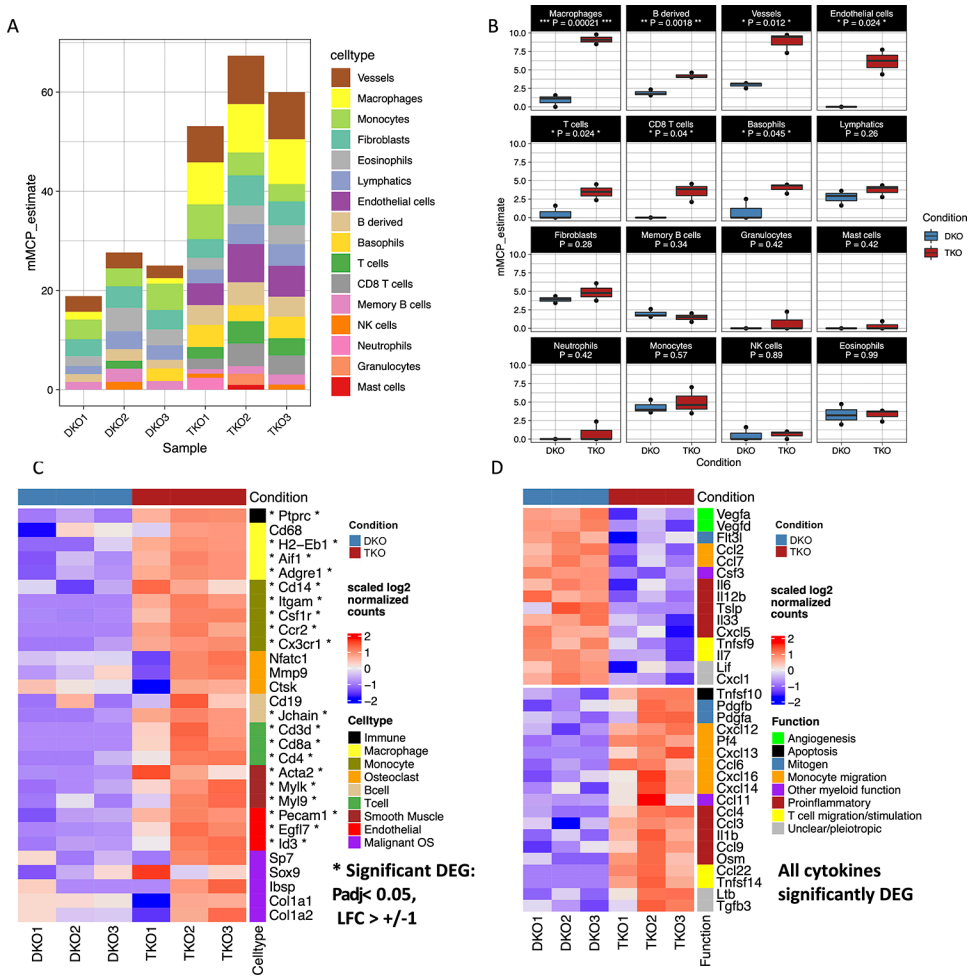

Figure 2: Microenvironment cell deconvolution analysis of bulk RNA-seq samples.

A): Barplots summarizing mMCP-Counter results for all cell types in each sample. **B**): Boxplots illustrating differential estimates of enrichment between TKO vs DKO. Asterisks (*) indicate statistical significance (t-test). **C**): Heatmap showing expression of specific markers of various infiltrating cell types. Asterisks (*) indicate statistically significantly differentially expressed genes between TKO vs DKO. **D**): Heatmap showing expression of differentially expressed cytokines.

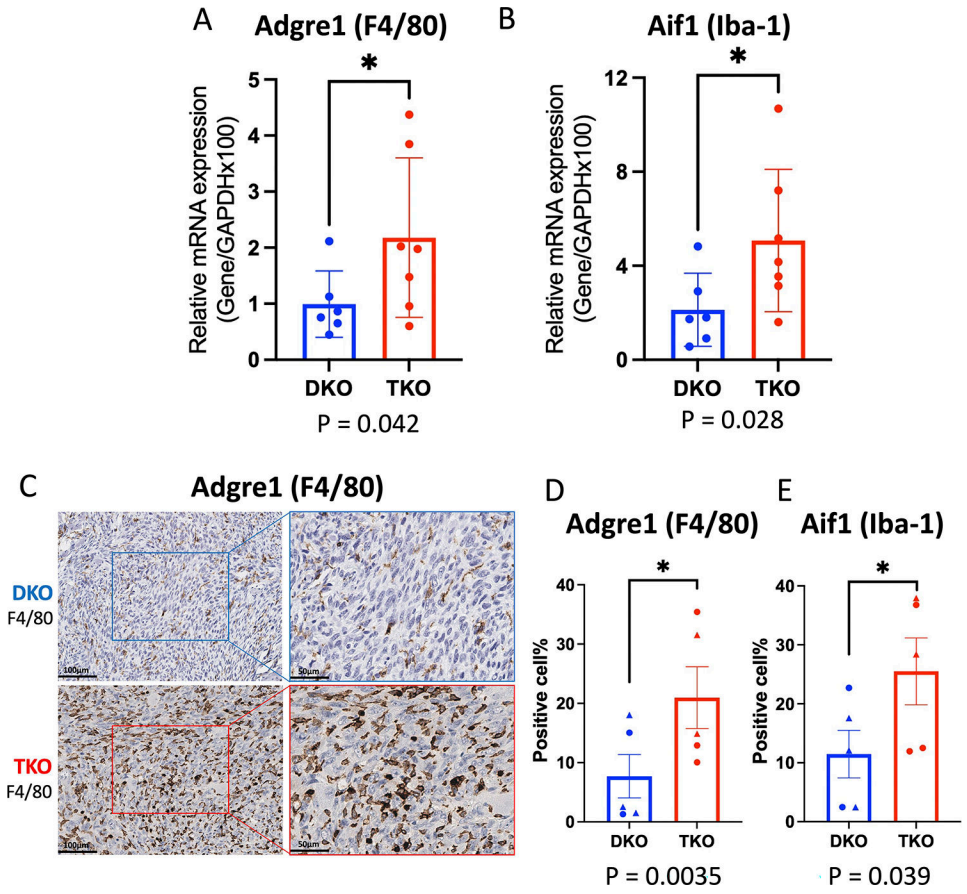

Figure 3: Validation of upregulation of macrophage markers in TKO

A,B): Quantitative PCR results for macrophage markers Adgre (F4/80) and Aif1 (Iba-1), respectively, in TKO vs DKO. All samples were not used in bulk RNA-seq. **C**): Representative image of immunohistochemistry (IHC) for macrophage marker Adgre1 (F4/80) staining in TKO vs DKO tumors. **D,E**): Quantification IHC-derived positive cell percentage and comparison for Adgre (F4/80) and Aif1 (Iba-1), respectively, in TKO vs DKO. Triangle points show tumors used in bulk RNA-seq, while circle points show new tumors.

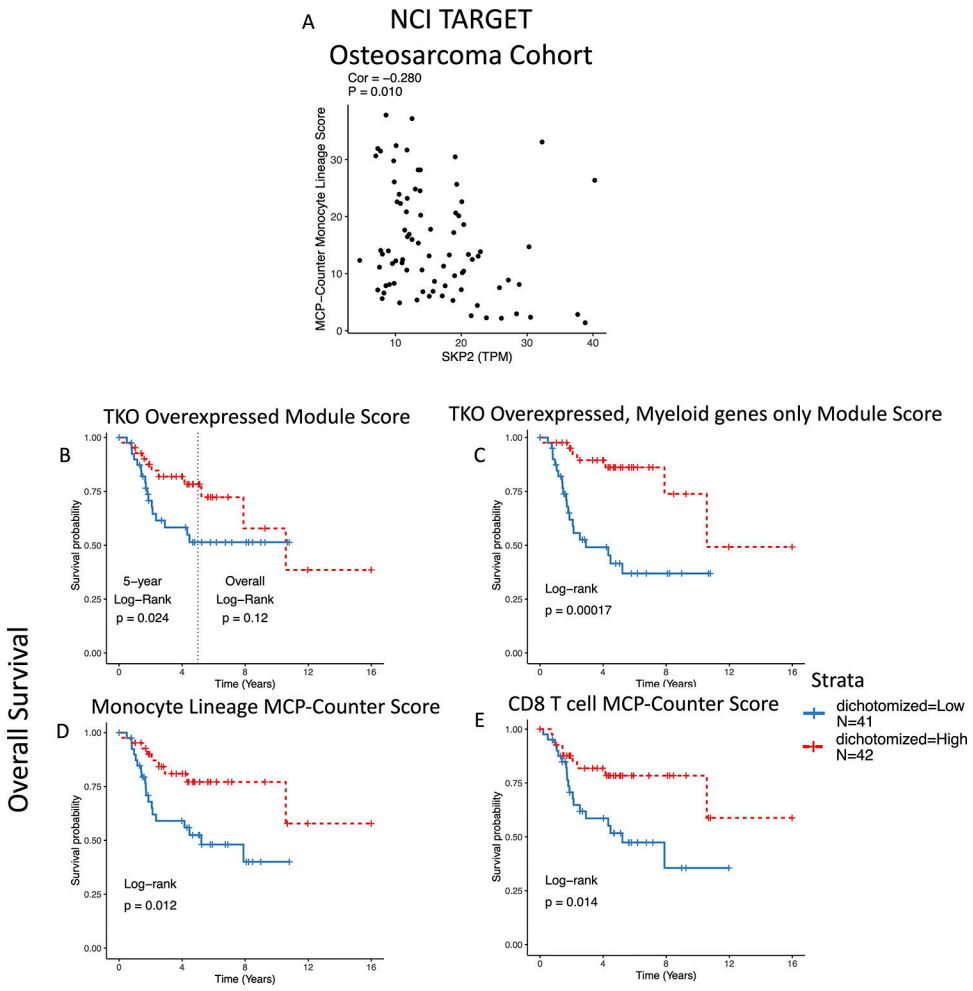

Figure 4: Correlations of up-regulated genes in *Skp2* KO tumors with macrophages and improved survival in patients.

A) SKP2 correlation with MCP-Counter monocyte lineage score for the TARGET OS cohort. **B-E**): Kaplan-Meier (KM) plots showing overall survival for patients from the NCI TARGET OS cohort with high versus low scores for the TKO upregulated gene module, the module of myeloid-only genes from the TKO upregulated signature, MCP-Counter monocyte lineage infiltration score, and MCP-Counter CD8 T cell score, respectively. For each variable, the cohort was dichotomized at the median to compare survival in high-score vs low-score patients.